This article was downloaded by: *[B-on Consortium - 2007]*
On: *11 January 2010*
Access details: *Access Details: [subscription number 908038079]*
Publisher *Taylor & Francis*
Informa Ltd Registered in England and Wales Registered Number: 1072954 Registered office: Mortimer House, 37-41 Mortimer Street, London W1T 3JH, UK

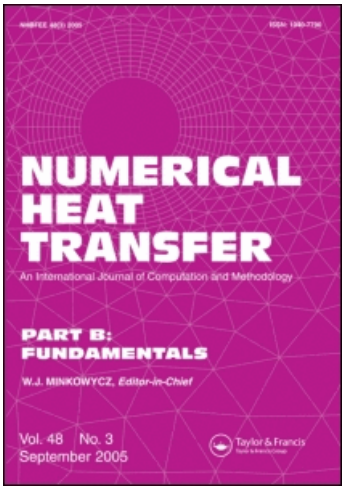

Numerical Heat Transfer, Part B: Fundamentals

Publication details, including instructions for authors and subscription information:
http://www.informaworld.com/smpp/title~content=t713723316

New Formulation for Stress Calculation: Application to Viscoelastic Flow in a T-Junction

H. M. Matos [a]; M. A. Alves [b]; P. J. Oliveira [a]
[a] Departamento de Engenharia Electromecânica, UMTP, Universidade da Beira Interior, Covilhã, Portugal [b] Departamento de Engenharia Química, CEFT, Faculdade de Engenharia da Universidade do Porto, Porto, Portugal

Online publication date: 11 January 2010

To cite this Article Matos, H. M., Alves, M. A. and Oliveira, P. J.(2009) 'New Formulation for Stress Calculation: Application to Viscoelastic Flow in a T-Junction', Numerical Heat Transfer, Part B: Fundamentals, 56: 5, 351 — 371
To link to this Article: DOI: 10.1080/10407790903507972
URL: http://dx.doi.org/10.1080/10407790903507972

PLEASE SCROLL DOWN FOR ARTICLE

Full terms and conditions of use: http://www.informaworld.com/terms-and-conditions-of-access.pdf

This article may be used for research, teaching and private study purposes. Any substantial or systematic reproduction, re-distribution, re-selling, loan or sub-licensing, systematic supply or distribution in any form to anyone is expressly forbidden.

The publisher does not give any warranty express or implied or make any representation that the contents will be complete or accurate or up to date. The accuracy of any instructions, formulae and drug doses should be independently verified with primary sources. The publisher shall not be liable for any loss, actions, claims, proceedings, demand or costs or damages whatsoever or howsoever caused arising directly or indirectly in connection with or arising out of the use of this material.

Numerical Heat Transfer, Part B, 56: 351–371, 2009
Copyright © Taylor & Francis Group, LLC
ISSN: 1040-7790 print/1521-0626 online
DOI: 10.1080/10407790903507972

Taylor & Francis
Taylor & Francis Group

NEW FORMULATION FOR STRESS CALCULATION: APPLICATION TO VISCOELASTIC FLOW IN A T-JUNCTION

H. M. Matos[1], M. A. Alves[2], and P. J. Oliveira[1]

[1]*Departamento de Engenharia Electromecânica, UMTP, Universidade da Beira Interior, Covilhã, Portugal*

[2]*Departamento de Engenharia Química, CEFT, Faculdade de Engenharia da Universidade do Porto, Porto, Portugal*

In this study, a new formulation is proposed for the calculation of stress components at control-volume faces, within the context of cell-centered finite-volume methods which have the stress tensor as one of the main dependent variables. Test case results from calculations with viscoelastic fluids flowing through a T-junction demonstrate the merits of the method. Previous formulations for stress interpolation yielded results that would depend on the time-step value employed, even when calculating steady-state problems. We have removed this inconsistency by devising an improved method that gives results independent of the time step and that in addition is more robust, with a wider range of allowable Deborah numbers. A FENE-CR constitutive model is used to replicate the known viscoelastic nature of blood, and results are given for varying fluid elasticities, at values of Reynolds number and extraction ratio typical of hemodynamic applications.

Downloaded By: [B-on Consortium - 2007] At: 18:42 11 January 2010

1. INTRODUCTION

In the simulation of steady flows with time-marching algorithms, the choice of the value of the time step (Δt) is important because it may be responsible for either convergence or divergence of the iterative solution method. In general, the use of small values for the time step facilitates the iterative convergence of the numerical method, but the CPU time taken to achieve converged results tends to become much longer. On the other hand, the choice of large values for the time step may be responsible for the divergence of the numeric method. However, often the formulations to calculate fluxes on nonstaggered grids are inconsistent, in the sense of providing solutions that depend on Δt even when simulating steady flows, and the above simple conclusions may not hold.

Received 27 January 2009; accepted 28 October 2009.

Financial support by Fundação para a Ciência e a Tecnologia (FCT, Portugal) through Ph.D. grant SFRH/BD/18062/2004 (M.H.H.) and project PTDC/EQU-FTT/71800/2006 (M.A.A.) is gratefully acknowledged. P.J.O. also acknowledges a sabbatical leave provided by Universidade da Beira Interior.

Address correspondence to M. A. Alves, Departamento de Engenharia Química, Faculdade de Engenharia da Universidade do Porto, Rua Dr. Roberto Frias, 4200-465 Porto, Portugal. E-mail: mmalves@fe.up.pt

NOMENCLATURE

a_F, a_P, a_0	coefficients, central coefficient, sum of neighbor coefficients
b_{li}	coefficients in stress equation that multiply velocity differences
B_{fi}	area components at cell face
De	Deborah number
$f(\tau)$	stress function in constitutive equation
H	channel height
$H(u)$, $H(\tau)$	neighbor contributions in algebraic equations (momentum and stress)
L^2	extensibility parameter in constitutive equation
n, $n+1$	time levels
p	pressure
Q	volumetric flow rate
r_x, r_y	mesh contraction/expansion ratios ($=\Delta x_{i+1}/\Delta x_i$, $\Delta y_{j+1}/\Delta y_j$)
Re	Reynolds number
S	source term
$\mathbf{u}$, u_i	velocity vector and Cartesian components
V	cell volume
x_i; x, y	Cartesian coordinates
X, Y	nondimensional coordinates
Δt	time step
Δp	pressure difference
$[\Delta u_i]_l$	velocity-component differences along direction l
λ	relaxation time
ρ	density
η	viscosity coefficient
τ, τ_{ij}	stress tensor and components

Superscripts

$'$	division by central coefficient
$-$	arithmetic or linear averaging
$\sim$	special cell face average
τ	stress equation

Subscripts

f	cell face
F	neighbor–cell center
i, j	Cartesian coordinates
l, f	direction, face direction (along curvilinear coordinates)
L	lengths of recirculation eddies
P	cell center position
s, p, 0	solvent, polymer, total (for viscosity)
1, 2, 3	T-junction inlet, main outlet, and branch outlet, respectively

In this article we are concerned with the computation of non-Newtonian flows requiring solution of additional evolution equations for the extra stress tensor, the so-called rheological equations of state. A key issue that arises when collocated finite-volume methods are applied is the evaluation of stress components at the control-volume faces, which are necessary for the approximation of the stress divergence term in the momentum equation. Oliveira et al. [1, 2] have addressed this issue and devised a method, inspired by the Rhie and Chow [3] interpolation for the convective fluxes, which has been applied successfully in a number of subsequent studies (e.g., Alves et al. [4]). They were not, however, concerned with the Δt dependence of the method, because it was then thought that the increased complexity of the formulation to avoid that problem would not compensate for the slight inconsistency. When the formulations used for the interpolation of stresses and convective fluxes at the control-volume faces are dependent on the time step employed, the choice of this numerical parameter becomes even more important because, besides the problems of inconsistency and lack of algorithm robustness, the value of Δt cannot be changed in a sequence of runs, or abrupt changes in the results may be provoked.

Dependence of a numerical solution on the time-step value, under steady-state conditions, is related to two factors: the formulation followed for the calculation of convective fluxes at control-volume faces, and the formulation for stress calculation at the control-volume faces. The former has been studied by several authors, starting with Majumdar [5] and Miller and Schmidt [6], who reported on the equivalent

Downloaded By: [B-on Consortium - 2007] At: 18:42 11 January 2010

problem of dependence on the underrelaxation parameter; Oliveira [7] and Issa and Oliveira [8], and later Choi [9], dealt with the Δt dependence. An additional point related to the fact that the original Rhie and Chow interpolation may still develop the unphysical pressure checkerboard pattern when Δt is small was noticed by Oliveira [7], who showed that the Δt-independent formulation offers also the additional benefit of avoiding this problem; this point was later independently rediscovered by Shen et al. [10] and Yu et al. [11]. Gu [12] and Choi [9] examined a similar question related to rapidly changing source terms, whose effect should be included in the face flux formulation; and recently Mencinger and Zun [13] revisited the problem, proposing a more effective treatment. This latter article is recommended reading, as it reviews the main aspects involved in evaluating face velocities on non-staggered grids: Mencinger and Zun also dealt with source terms arising from curvature and surface tension in free-surface flows, but it is worth mentioning that treatment of source terms proportional to gradients of some variable were previously correctly addressed by Kunz et al. [14] and by Oliveira and Issa [15]. Development of new formulations, independent of the time-step value, for the interpolation of stresses and convective flux at the control-volume faces is the scope of the present article.

The geometry chosen to test the independence of Δt for the several formulations proposed is a two-dimensional, 90° bifurcation. Simulation of laminar flows through bifurcations (e.g., [8, 16–19]) is of enormous practical importance, since bifurcations are present in many situations with relevance for engineering and human health. Examples of the latter occur in hemodynamic applications, such as in the human circulatory system, where blood drains along successive bifurcations and junctions of arteries and veins. Although the rheological behavior of blood in the large vessels is adequately approximated by Newtonian or generalized Newtonian models, it is known that blood exhibits non-Newtonian characteristics when flowing in smaller-diameter vessels, which are enhanced under the unsteadiness imposed by the heart beats; in particular, blood viscoelasticity then becomes important [20]. For this reason, in the present work we will use two forms of the finite-extensibility nonlinear dumbbell model [21] as an approximation to represent blood behavior, and we will look into the influence of elasticity on viscoelastic flow through a T-junction, for values of Reynolds number and extraction ratio typical of the human circulatory system. A motivation for this study is that cardiovascular diseases, such as atherosclerosis and thrombosis, are associated with complex flows in the human circulatory system and are usually located near side branches of bifurcations and on the inner curvatures of arteries [22]. The study is thus a continuation of a previous work [19], which was concerned with the behavior of steady and unsteady laminar flow, with Newtonian and non-Newtonian inelastic fluids, for the same test case.

The main objectives of this work are therefore (1) to develop new formulations for the interpolation of stresses and convective flux at the control-volume faces that will provide numerical solutions independent of the time-step size, and study the robustness of these formulations in order to verify which are the best options to use for Newtonian or non-Newtonian viscoelastic flow simulations; (2) to investigate, by means of numerical simulations, steady laminar flow in a planar two-dimensional T-junction with fluids that possess viscoelastic properties (with characteristics adjusted to those of human blood).

Downloaded By: [B-on Consortium - 2007] At: 18:42 11 January 2010

2. GOVERNING EQUATIONS

Incompressible and isothermal laminar flow of a polymeric solution is governed, as usual, by conservation equations for mass and linear momentum:

$$\nabla \cdot \mathbf{u} = 0 \tag{1}$$

$$\rho \frac{D\mathbf{u}}{Dt} = -\nabla p + \nabla \cdot \boldsymbol{\tau} + \nabla \cdot (2\eta_s \mathbf{D}) \tag{2}$$

where $\mathbf{u}$ is the velocity vector, p is the pressure, ρ is the fluid density, $\mathbf{D} = (\nabla\mathbf{u} + \nabla\mathbf{u}^T)/2$ is the rate-of-strain tensor, and η_s is the solvent viscosity. In this study, the fluid density and the total viscosity $\eta_0 = \eta_s + \eta_p$, where η_p is the polymeric viscosity contribution, are assumed constant.

Solution of Eq. (2) requires an additional equation for the evolution of the non-Newtonian contribution to the extra stress tensor $\boldsymbol{\tau}$. For that purpose, two rheological constitutive models derived from the finitely extendable nonlinear dumbbell model (FENE [21]) are employed: the FENE-CR and the FENE-MCR constitutive equations. In the FENE-CR model proposed by Chilcot and Rallison [23], the stress tensor is expressed by

$$\boldsymbol{\tau} + \lambda \left(\frac{\overset{\triangledown}{\boldsymbol{\tau}}}{f(\boldsymbol{\tau})} \right) = 2\eta_p \mathbf{D} \tag{3}$$

where λ is the relaxation time of the fluid. The symbol $\triangledown$ denotes Oldroyd's upper-convected derivative:

$$\overset{\triangledown}{\boldsymbol{\tau}} = \frac{D\boldsymbol{\tau}}{Dt} - (\nabla\mathbf{u}^T \cdot \boldsymbol{\tau} + \boldsymbol{\tau} \cdot \nabla\mathbf{u}) \tag{4}$$

where the superscript T means the transposed tensor and $D(\,)/Dt \equiv \partial(\,)/\partial t + \mathbf{u} \cdot \nabla(\,)$ is the material derivative. In Eq. (3) the function of invariants of $\boldsymbol{\tau}$, $f(\boldsymbol{\tau})$, is defined as

$$f(\boldsymbol{\tau}) = \frac{L^2 + (\lambda/\eta_p)\,\mathrm{Tr}(\boldsymbol{\tau})}{L^2 - 3} \tag{5}$$

where L^2 is the maximum extensibility of the dumbbells, a model parameter which is kept constant in the simulations for both models ($L^2 = 100$), and Tr represents the trace operator. If the additional simplification $Df(\boldsymbol{\tau})/Dt \approx 0$ is assumed in Eq. (3), then the modified FENE-CR model is obtained (FENE-MCR), which was used by Coates et al. [24] among others:

$$\boldsymbol{\tau} + \frac{\lambda}{f(\boldsymbol{\tau})} \overset{\triangledown}{\boldsymbol{\tau}} = 2\eta_p \mathbf{D} \tag{6}$$

Both the FENE-CR and FENE-MCR models give identical responses in simple steady shear and elongational flows; the only differences between the two models occur in transient flows and in strongly convective flows, where the term

Downloaded By: [B-on Consortium - 2007] At: 18:42 11 January 2010

neglected in the FENE-MCR model ($\mathbf{u} \cdot \nabla(1/f)$) may be significant. Those models, and the form of the respective constitutive equations [Eqs. (3) and (6)], are typical in non-Newtonian fluid mechanics of viscoelastic fluids, and more complex models follow the same type of equation but with many additional terms. They serve well the purpose of deriving better formulations for the stresses arising from the divergence term in Eq. (2).

3. NUMERICAL METHOD

The differential equations of the previous section are discretized using the finite-volume method [25, 26]. In the present implementation of the method [7], general coordinates and indirect addressing for easy mapping of nonrectangular domains are used together with nonstaggered meshes in which all variables are stored at the centers of the control volumes. In order to ensure an adequate coupling between the velocity and pressure fields in these types of meshes, we follow the interpolation technique of Rhie and Chow [3] to evaluate the velocity components at the cell faces, while the coupling between the stress and the velocity fields is obtained using a somewhat similar procedure, which was described in [1, 2]. These are the procedures we intend to improve in this study.

The diffusive and the pressure gradient terms in the governing equations are represented by central differences (second-order accuracy), while the convective terms are approximated by the high-resolution scheme CUBISTA of Alves et al. [27]. This scheme possesses good accuracy (third-order accuracy in space for smooth flow) complemented with improved characteristics regarding iterative convergence in viscoelastic flows, as demonstrated in [27].

The solution algorithm is based on the SIMPLEC [28] a well-known version of the pressure-correction methodology for dealing with the coupling of the velocity and pressure fields in order to verify the continuity equation. Convergence of the iterative, time-marching process is obtained when the normalized residuals of all variables are less than 10^{-8}. The choice of such a small value is justified by the fact that we want to make sure the solutions are independent of the time step, and that cannot be guaranteed with the usual stopping tolerance for the normalized residuals (of about 10^{-4}), especially when elasticity is appreciable (Deborah numbers above $\mathrm{De} \approx 1$).

As mentioned in the Introduction, several formulations may be devised for the calculation of the convective fluxes and stresses at the control-volume faces. For future convenience we will designate the formulations for calculation of convective fluxes at the faces of control volumes by formulations of type *F*, and those for the stress calculation at the faces of control volumes by formulations of type *T*. The final formulation used in practice is a combination of these two types, *F* and *T*.

3.1. Formulations for the Convective Fluxes (Type *F*)

For the calculation of convective fluxes, two formulations were employed. The first (*F1*) was used in previous simulations and leads to solutions that are dependent of the value of the time step Δt, for both Newtonian and non-Newtonian flows. The second formulation for the convective fluxes calculation (*F2*) was proposed in [7] (see also [8]) and promotes steady-state solutions that do not depend on Δt.

Downloaded By: [B-on Consortium - 2007] At: 18:42 11 January 2010

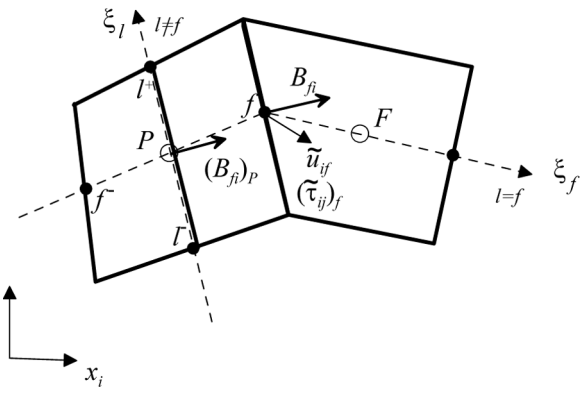

Figure 1. Two-dimensional scheme of a general control volume P and its neighbor cell F across face f with additional notation.

Downloaded By: [B-on Consortium - 2007] At: 18:42 11 January 2010

The two formulations for the convective fluxes calculation differ in how the velocity components at the control-volume faces are obtained from the discretized momentum equation (see Figure 1):

$$a_P u_P = H(u) - B\ \Delta p + \frac{\rho V_P}{\Delta t} u_P^n \tag{7}$$

where u_p is the velocity at the center of the cell P, $H(u) = \sum a_F u_F + S_u$, where the index F is related to the neighboring cells of P, and S_u represents source terms other than the pressure gradient, B is a superficial area, Δp is a difference of pressures across the cell, V is the volume of the cell, and u^n is the velocity at the present time level (iteration). Since the inertial term is retained in Eq. (2), being discretized with a simple, full implicit Euler scheme when the interest is to obtain steady-state solutions, the central coefficient in Eq. (7) is given by $a_P = a_0 + \rho V_P/\Delta t$, where $a_0 = \sum a_F$ contains the usual convective and diffusive contributions. For simplicity of presentation, we do not include the Cartesian index to denote the velocity component in Eq. (7) and the other equations in this subsection; on general curvilinear grids the discretized pressure gradient term, for example, should be written as $B\ \Delta p = \sum_l B_{li}[\Delta p]_l^P$, with $l = 1, 2, 3$ for the three directions. Further notation is clarified in Figure 1.

3.1.1. Flux formulation *F1*. We follow the technique suggested by Rhie and Chow [3] and, instead of determining the face velocity from arithmetic averaging (denoted here with overbar) of Eq. (7),

$$\overline{a_P u_P} = \overline{H(u)} - \overline{B\ \Delta p} + \overline{\frac{\rho V}{\Delta t} u^n} \tag{8}$$

we write an equation similar to this except that the term related to the pressure gradient is obtained directly at the face of the control volume:

$$\overline{a_P}\tilde{u}_f = \overline{H(u)} - B_f \widetilde{\Delta p_f} + \overline{\frac{\rho V}{\Delta t} u^n} \tag{9}$$

The index f refers to conditions at the control-volume face, and the tilde denotes the particular "Rhie and Chow" type of interpolation defined by Eq. (9); the pressure difference calculated at the face is $\widetilde{\Delta p_f} = p_F - p_P$, where F is the neighbor cell across face f, whose area is B_f (see Figure 1). Subtracting Eq. (8) from Eq. (9), we obtain the equation for the control-volume face velocity, $\widetilde{u_f}$:

$$\widetilde{u_f} = \frac{\overline{a_p u_p} - B_f \widetilde{\Delta p_f} + \overline{B \Delta p}}{\overline{a_p}} \tag{10}$$

Since $\overline{a_p} = (\overline{a_0} + \overline{\rho V / \Delta t})$, the velocity at the control-volume face will in general depend on the particular value of the time step (Δt), thus explaining the time-step dependence registered for this formulation. Some authors (e.g., Ferziger and Peric [26], p. 202) argue that the terms in Δt in Eq. (10) that bring in the inconsistency are of the order of the discretization error, and so the dependence of the solution on Δt (or underrelaxation parameter) is not important. Others (e.g., Majumdar [5]) have addressed this issue and devised formulations that avoid this inconsistency. One such formulation is explained next.

3.1.2. Flux formulation *F2*. Regarding its derivation, formulation *F2* has just a small difference compared to formulation *F1*. Instead of using Eq. (9) to define the face velocity $\widetilde{u_f}$, we define it by

$$\overline{a_p} \widetilde{u_f} = \overline{H(u)} - B_f \widetilde{\Delta p_f} + \frac{\overline{\rho V}}{\Delta t} \widetilde{u_f^n} \tag{11}$$

where the face velocity calculated at the present time level $\widetilde{u_f^n}$ is now also obtained by Rhie and Chow's technique. This slight modification was proposed by Oliveira [7], and it is sufficient to guarantee Δt-independent solutions, contrary to what was claimed by Yu et al. [29]; the proposals to avoid Δt dependence later reported in [9, 10, 29, 30] follow the same type of ideas as [7, 8]. In the same way as before, by subtracting Eq. (8) from Eq. (11), we obtain the equation for the velocity at the control-volume faces, $\widetilde{u_f}$:

$$\widetilde{u_f} = \frac{\overline{a_p u_p} - B_f \widetilde{\Delta p_f} + \overline{B \Delta p} + \left(\overline{\frac{\rho V}{\Delta t}}\right) \widetilde{u_f^n} - \overline{\frac{\rho V}{\Delta t} u^n}}{\overline{\left[a_0 + \left(\frac{\rho V}{\Delta t}\right)\right]}} \tag{12}$$

In this case it is easy to verify that when a steady state is reached, the value of the velocity at the control-volume faces $\widetilde{u_f}$ will not depend on the time step value Δt. In fact, when the iterative process has converged to steady state, velocities will no longer change and we have $\widetilde{u_f} = \widetilde{u_f^n}$ and $u_P = u_P^n$; thus the terms in Eq. (12) containing Δt will mutually cancel out, leaving just the steady state expression for the face velocity,

$$\widetilde{u_f}_\infty = \frac{\overline{a_0 u_p} - B_f \widetilde{\Delta p_f} + \overline{B \Delta p}}{\overline{a_0}} \tag{13}$$

which is free of any Δt dependence. As alluded to above, the proposals of [9–12, 29, 30] are essentially equivalent to this formulation except in details. One difference worth

Downloaded By: [B-on Consortium - 2007] At: 18:42 11 January 2010

mentioning is that most authors prefer to work with linear interpolation of velocity itself, an intensive property, while we interpolate momentum, the quantity which is in fact conserved; since momentum is an extensive property, the interpolations denoted with overbars in the previous equations must be arithmetic averages (even for nonuniform mesh spacing).

3.2. Formulations for the Stress Calculation (Type *T*)

For the calculation of stress at the control-volume faces, we discuss three formulations; one of them is a new formulation devised in order to obtain results independent of the time step and provide a more robust algorithm.

In any case, the cell-face stresses are obtained by a suitable interpolation of the discretized equations for cell-center stresses. Any spatial discretization scheme applied to either Eq. (3) or Eq. (6), together with the temporal implicit Euler scheme, ends up with linearized algebraic equations of the form (see [1] for details)

$$a_P^{\tau}\tau_{ijP} = H^{\tau}(\tau_{ij}) + \sum_{l=1}^{3}(b_{li}[\Delta u_j]_l + b_{lj}[\Delta u_i]_l) + \frac{\lambda_{ef}V_P}{\Delta t}\tau_{ijP}^{n} \tag{14}$$

where

$$\begin{aligned} a_P^{\tau} &= a_0^{\tau} + V + \frac{\lambda_{ef}V}{\Delta t} \qquad a_0^{\tau} = \sum a_F^{\tau} \qquad H^{\tau} = \sum a_F^{\tau}\tau_{ijF} + S_{\tau} \\ b_{li} &= \eta_p B_{li} + \lambda_{ef}\sum_k B_{lk}\tau_{ki} \qquad \lambda_{ef} = \frac{\lambda}{f(\tau)} \end{aligned} \tag{15}$$

The coefficients of the stress equations a_F^{τ} contain only convective influences, and the source term S_{τ} contains contributions not accounted for by the other source terms written explicitly in Eq. (14), which are the time-dependent term and all velocity-gradient terms in the constitutive equations. These latter terms are included in the b_{li} terms of Eq. (14), where the velocity differences at cell center are evaluated with linearly interpolated velocities, $[\Delta u_i]_l = \overline{u_i^{l+}} - \overline{u_i^{l-}}$ ($l = 1, 2, 3$ is any of the three general coordinate directions; l^+ (l^-) is the cell face lying on the positive (negative) l direction; see Figure 1).

3.2.1. Stress formulation *T1*. In this formulation the expressions for the cell-face stress calculation are obtained from linear interpolation of the discretized stress constitutive equation, Eq. (14), except for the terms proportional to velocity differences straddling the face, which are evaluated directly at the face. This procedure is described in detail in [2] and guarantees that decoupling problems between stress and velocity fields will not exist. Formulation *T1* is expressed by Eq. (16) and by the auxiliary relationships of Eq. (17), where the prime notation designates in general a division by the central coefficient of the discretized stress equation.

$$(\widetilde{\tau_{ij}})_f = (\overline{\tau_{ij}})_f + \{(\widetilde{b'_{fi}}\,[\Delta u_j]_f + \widetilde{b'_{fj}}[\Delta u_i]_f) - \overline{(b'_{fi}[\Delta u_j]_f + b'_{fj}[\Delta u_i]_f)}\} \tag{16}$$

Downloaded By: [B-on Consortium - 2007] At: 18:42 11 January 2010

where

$$b'_{fi} = \frac{\eta_p B_{fi} + \lambda_{ef} \sum_k B_{fk} \tau_{ki}}{a_P^\tau} \qquad \text{and} \qquad \widetilde{b'_{fi}} = \frac{\left(\eta_p B_{fi} + \lambda_{ef} \sum_k B_{fk} \overline{\tau_{ki}} \right)_f}{V_f \overline{(a_P^\tau / V_P)}} \tag{17}$$

In these equations, B_{fi} is the i component of the cell face area aligned with the direction f, V_P and V_f are the volumes of the cell centered at P and at the face f. The superscript ($\sim$) is used to denote the special Rhie and Chow type of interpolation devised by [2] for the stresses, while the overline (–) corresponds here to linear interpolation [$\overline{\phi}_f = w_f \phi_F + (1 - w_f)\phi_P$ where w_f is a geometric weighting factor $w_f = \Delta s_P / (\Delta s_P + \Delta s_F)$, with s representing a local coordinate]. As the central coefficient a_P^τ is given by $a_P^\tau = \lambda_{ef} V_P / \Delta t + V_P + a_0^\tau$ (cf. Eq. (15)), this formulation for the stress calculation will produce results that, when converged (stationary solution), will depend on the value of the time step Δt. The formulation defined by Eq. (16) is thus somewhat "inconsistent," in the sense discussed before for the face velocity [cf. Eq. (12)], because the terms containing Δt do not cancel out mutually under steady flow conditions and a Δt dependence will persist.

3.2.2. Stress formulation *T2*. The second formulation is a new proposal devised during the course of the present work, resulting from a simplification of formulation *T1* described previously, with the objective of obtaining results that are independent of the time-step value. After a number of numerical experiments with several possible formulations which we shall omit here for the sake of conciseness, we arrived at the following "optimized" expression for the stress calculation:

$$(\widetilde{\tau_{ij}})_f = (\overline{\tau_{ij}})_f + \frac{1}{\overline{(1 + a_0^\tau / V)}} \left[\frac{1}{V_f} (\eta_p B_{fi} [\Delta u_j]_f + \eta_p B_{fj} [\Delta u_i]_f) - \overline{\frac{1}{V} (\eta_p B_{fi} [\Delta u_j]_f + \eta_p B_{fj} [\Delta u_i]_f)} \right] \tag{18}$$

A "formal" derivation leading to Eq. (18) would start by rewriting Eq. (14) as

$$V \left(1 + \frac{a_0^\tau}{V} \right) \tau_{ijP} = \eta_p \sum_{l=1}^{3} (B_{li} [\Delta u_j]_l + B_{lj} [\Delta u_i]_l) + H^\tau(\tau_{ij}) + \lambda_{ef} \sum_{l=1}^{3} (T_{li} [\Delta u_j]_l + T_{lj} [\Delta u_i]_l) + \frac{\lambda_{ef} V_P}{\Delta t} (\tau_{ijP}^n - \tau_{ijP}) \tag{19}$$

where the traction vector is defined by $T_{li} = \sum_k B_{lk} \tau_{ki}$. Now, after division of (19) by the cell volume in order to end up with intensive properties (stresses instead of forces), the face stress is defined by linear interpolation (overbar) of all terms on the right-hand side, except those in the first summation for the direction of the face

Downloaded By: [B-on Consortium - 2007] At: 18:42 11 January 2010

$l=f$, that is,

$$\overline{\left(1+\frac{a_0^\tau}{V}\right)}(\widetilde{\tau_{ij}})_f = \frac{\eta_p}{V_f}(B_{fi}[\Delta u_j]_f + B_{fj}[\Delta u_i]_f) + \eta_p \sum_{l\neq f}^{2} \overline{\frac{1}{V}(B_{li}[\Delta u_j]_l + B_{lj}[\Delta u_i]_l)} + \overline{\frac{1}{V}H^\tau(\tau_{ij})} + \sum_{l=1}^{3} \overline{\frac{\lambda_{ef}}{V}(T_{li}[\Delta u_j]_l + T_{lj}[\Delta u_i]_l)} + \overline{\frac{\lambda_{ef}}{\Delta t}(\tau_{ijP}^n - \tau_{ijP})} \tag{20}$$

Finally, the incremental formulation (18) is obtained after applying linear interpolation to Eq. (14) and subtracting the resulting equation from Eq. (20) given above.

A few comments are necessary in order to provide some justification for this choice. In relation to formulation *T1* defined by Eq. (16), two points are noteworthy:

1. The local time derivative term of the constitutive equation, $\partial\tau_{ij}/\partial t$, was linearly interpolated, thus being effectively removed from the final expression for the face stress, which does not contain any terms in Δt; note that in Eqs. (16) and (17), terms in Δt are contained in the coefficient a_P^τ.
2. The rotation/deformation terms of the upper-convected derivative [the term between parenthesis in Eq. (4)] were also removed from the definition of the special interpolation for the stresses at the cell face$(\widetilde{\tau_{ij}})_f$.

Point 1 has the immediate consequence that the results become independent of the time step employed in the computations. Point 2 is justifiable on the basis that turning off a strong influence of viscoelasticity (note that the term removed is multiplied by the relaxation time of the fluid) results in a notable improvement in numerical stability, as Section 5 will demonstrate. Note that in the definition of the face stress, as explained above, linear interpolation from cell centers to cell faces is applied to all terms except those that are proportional to velocity gradients $\eta_p\nabla\mathbf{u}$, which are evaluated directly at the cell face in the spirit of Rhie and Chow. In the Left-hand side of the discretized equation (14), only the convective contribution (proportional to a_0^τ) and the term in τ [the first term in Eqs. (3) and (6)] are subject to the Rhie and Chow treatment. The central coefficient in the equation used to define the face stresses [the denominator in Eq. (18)] needs to be "large" to promote stability, and the inclusion of the latter term is justified in order to obtain a formulation that is valid for Newtonian calculations.

3.2.3. Stress formulation *T3*. The last formulation consists of a drastic simplification in which the stress components at the control-volume faces are obtained simply by linear interpolation of stresses at the neighboring control volumes. This formulation is thus defined by

$$(\widetilde{\tau_{ij}})_f = (\overline{\tau_{ij}})_f \tag{21}$$

Downloaded By: [B-on Consortium - 2007] At: 18:42 11 January 2010

Table 1. Summary of the formulations tested

Formulation name	Formulation for the convective fluxes	Formulation for the cell-face stress	Time-step dependence
Standard	*F2*	*T1*	Yes
Modified	*F2*	*T2*	No
Linear interpolation	*F2*	*T3*	No

3.3. Global Formulations Used in Practice

By combining the formulations for fluxes of Section 3.1 with the formulations for the face stresses of Section 3.2, we would end up with a large number of global formulations to be tested. In practice, only a few of them offer interesting results in terms of Δt independence and robustness, and we shall concentrate on these. In Table 1 we summarize the designation of the formulations effectively tested in the current work and provide the respective theoretical time-step dependence.

The objective of the work was not to test various rheological models, and therefore, as a matter of simplicity, most simulations carried out for the assessment of the various formulations indicated in Table 1 will use the FENE-MCR model; the new, modified formulation is the exception, and both rheological models, FENE-CR and FENE-MCR, will be included in the assessment.

4. GEOMETRY, COMPUTATIONAL MESHES, AND ACCURACY TESTS

The numerical simulations were done under conditions similar to those of Khodadadi et al. [17], with a T geometry (Figure 2) having a constant, rectangular cross-sectional area, where the height of the channels is $H = 0.01\,\text{m}$. Owing to the topology of the geometry, the computational mesh to map the calculation domain was generated by blocks. In the present work the mesh was prepared from six structured blocks (B1–B6), as represented in Figure 2, and the coordinate axes are centered in the bifurcation zone (block B2).

Boundary conditions encompassed one inlet, two outlets, and solid walls. Flow inlet is through the left face of block 1 (B1) at $x = -3.5H$, where a parabolic velocity profile is imposed having an average velocity of $u_1 = 0.0745\,\text{m/s}$. Outlets are located at $x = 22.5H$ (in block B5) and $y = 20.5H$ (in block B6), where conditions of vanishing axial variation were imposed for all quantities (i.e., $\partial/\partial x = 0$ in the horizontal duct and $\partial/\partial y = 0$ in the vertical duct), except pressure, for which a constant gradient was assumed, and the boundary value obtained by linear extrapolation from inside. Outlet channel lengths are sufficiently long to avoid flow disturbances in the junction region for the Reynolds number and extraction ratio tested, with $L_2 = 22H$ and $L_3 = 20H$ as in [19]. The remaining boundary faces of the geometry correspond to solid walls, where the no-slip boundary condition is imposed and the stresses are obtained from local analytical expressions.

Following Khodadadi et al. [17], the flow rate ratio was set at $\beta \equiv Q_3/Q_1 = 0.7$, where Q_1, Q_2, and Q_3 are, respectively, the volumetric flow rates at the inlet, the main branch outlet, and the secondary branch outlet, as represented in Figure 2. Imposition of the flow rate ratio β constitutes an additional boundary condition

Downloaded By: [B-on Consortium - 2007] At: 18:42 11 January 2010

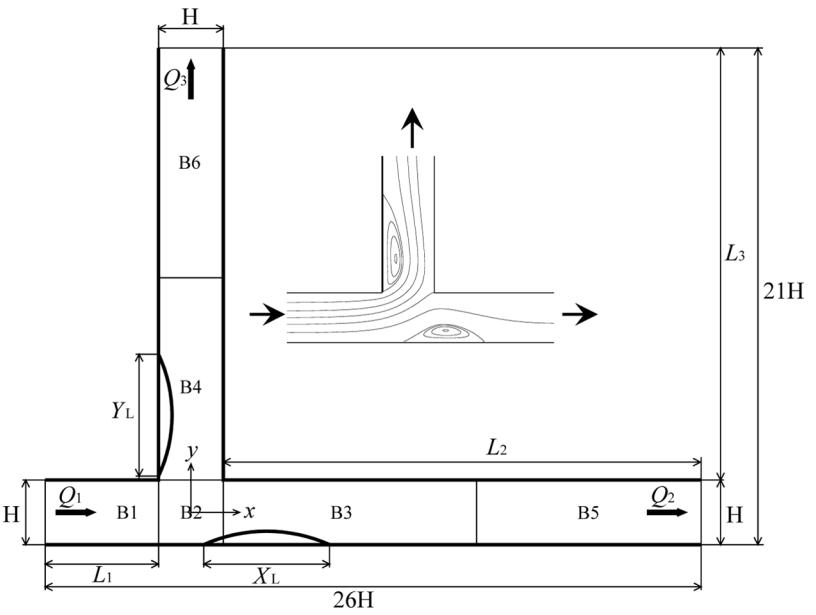

Figure 2. Schematic representation of the test section with illustrative streamline pattern (De = 0).

in bifurcation flows that must be applied to guarantee a unique solution to the governing equations. Simulations were carried out for a Newtonian fluid and three viscoelastic fluids with Deborah numbers equal to 1, 2.5, and 5. The controlling parameters are the Reynolds and the Deborah numbers, defined as

$$\mathrm{Re} = \frac{\rho u_1 H}{\eta_0} = 102 \qquad \mathrm{De} = \frac{\lambda u_1}{H} \tag{22}$$

with fluid density $\rho = 1{,}150\,\mathrm{kg/m^3}$ and viscosity $\eta_0 = 0.0084\,\mathrm{Pa}\cdot\mathrm{s}$. In the case of the viscoelastic fluids, the ratio between solvent viscosity and total viscosity is 0.80, giving a solvent viscosity $\eta_s = 0.0067\,\mathrm{Pa}\cdot\mathrm{s}$ and a polymeric viscosity $\eta_p = 0.0017\,\mathrm{Pa}\cdot\mathrm{s}$.

The mesh is orthogonal but nonuniform, with increased concentration of cells near the bifurcation zone, where the stress gradients are expected to be higher. A study of mesh convergence was based on three meshes having progressive degrees of refinement. The coarsest mesh M1 has 3,200 control volumes, while the most refined mesh M3 has 51,200 control volumes. In Table 2 we summarize the characteristics of the intermediate mesh M2, with 12,800 control volumes, which is the base mesh in this study because it provides adequate numerical accuracy. In order to have consistent mesh refinement, the most refined mesh is obtained from the previous mesh by doubling the number of cells along each direction and using the square root of the corresponding expansion/contraction ratios inside each bock. With these conditions, Richardson extrapolation technique can be applied directly, allowing calculation of the order of convergence of the method (p) and estimation of a more accurate solution on the basis of the values obtained on meshes with three different

Downloaded By: [B-on Consortium - 2007] At: 18:42 11 January 2010

Table 2. Main characteristics of the intermediate mesh M2

Block	Number of cells $NX \times NY$	Size X	Size Y	r_x	r_y
B1	40×40	$-3.5 \rightarrow -0.5$	$-0.5 \rightarrow +0.5$	0.95260	1.00000
B2	40×40	$-0.5 \rightarrow +0.5$	$-0.5 \rightarrow +0.5$	1.00000	1.00000
B3	100×40	$0.5 \rightarrow 12.5$	$-0.5 \rightarrow +0.5$	1.02657	1.00000
B4	40×100	$-0.5 \rightarrow +0.5$	$0.5 \rightarrow 10.5$	1.00000	1.02385
B5	20×40	$12.5 \rightarrow 22.5$	$-0.5 \rightarrow +0.5$	1.06413	1.00000
B6	40×20	$-0.5 \rightarrow +0.5$	$10.5 \rightarrow 20.5$	1.00000	1.06413

refinement levels. The order of convergence of the method is given by [26]

$$p = \frac{\log[(\phi_{2h} - \phi_{4h})/(\phi_h - \phi_{2h})]}{\log 2} \tag{23}$$

where ϕ is a representative solution functional and $4h$, $2h$, and h are, respectively, the characteristic spacing of meshes M1, M2, and M3 (their $\Delta x_{\min}$). A more accurate, extrapolated solution can be obtained through the expression [26]

$$\phi_{\text{extr}} \approx \phi_h + \varepsilon_h = \phi_h + \frac{\phi_h - \phi_{2h}}{2^p - 1} \tag{24}$$

where ε_h is the estimated error on the most refined mesh (M3).

In Table 3, we summarize the discretization errors on the three meshes for the calculation of the horizontal and vertical recirculation lengths, using the modified formulation and the FENE-MCR constitutive model, for two cases: $\text{De} = 0$ (Newtonian) and $\text{De} = 2.5$ (viscoelastic). A more accurate solution is also given, estimated by extrapolation, and the order of convergence obtained with Richardson's technique is also provided. From the results in Table 3 we can verify that the solution on the intermediate mesh M2 is close to the reference solution obtained using Richardson's extrapolation technique. We have therefore chosen mesh M2 for the remaining simulations of the present work, in detriment of mesh M3 due to the high CPU times involved with this most refined mesh.

Table 3. Summary of the errors obtained with the various meshes using the Modified formulation

	$\text{De} = 0$		$\text{De} = 2.5$	
	X_L	Y_L	X_L	Y_L
Mesh M1	1.52410	1.90309	1.49743	1.73787
Mesh M2	1.53367	1.95232	1.47461	1.88648
Mesh M3	1.53475	1.96689	1.46957	1.94449
p	3.15	1.76	2.18	1.36
ϕ_{extr}	1.53489	1.97301	1.46814	1.98163
ε_{4h} (M1)	0.70%	3.54%	1.99%	12.3%
ε_{2h} (M2)	0.079%	1.05%	0.44%	4.80%
ε_h (M3)	0.0091%	0.31%	0.097%	1.87%

Downloaded By: [B-on Consortium - 2007] At: 18:42 11 January 2010

5. RESULTS AND DISCUSSION

All results are given under nondimensional form, using as length scale the channels height H ($Y = y/H$ and $X = x/H$), as velocity scale the average velocity of the inlet flow (u_1), as stress scale the value of the wall shear stress at the inlet under fully developed steady flow ($\tau_{w1} = 6\eta_0 u_1/H$), and as time scale the ratio H/u_1. Results related to the numerical formulations, namely, the Δt dependence and algorithm robustness, are discussed first (Section 5.1), and then the physical aspects of the results for viscoelastic flow in the T-junction are addressed (Section 5.2), in particular, the influence of elasticity on the size and intensity of the eddies and the stress fields.

5.1. Assessment of Δt Dependence

Figures 3 and 4 give the predicted results for the lengths of the recirculating eddies formed along the x and y directions, obtained from velocity profiles parallel to the horizontal ($Y = -0.5$) and vertical ($X = -0.5$) walls, for the various formulations and fluids considered. These figures illustrate the possible dependence of the numerical solution on the time-step values. It is emphasized that the time steps Δt are nondimensional (scaled with H/u_1), and for the Newtonian case iterative convergence can be achieved for quite large values of Δt (up to $\Delta t \approx 5$), a feature that may be explained by the fully implicit nature of the solution algorithm.

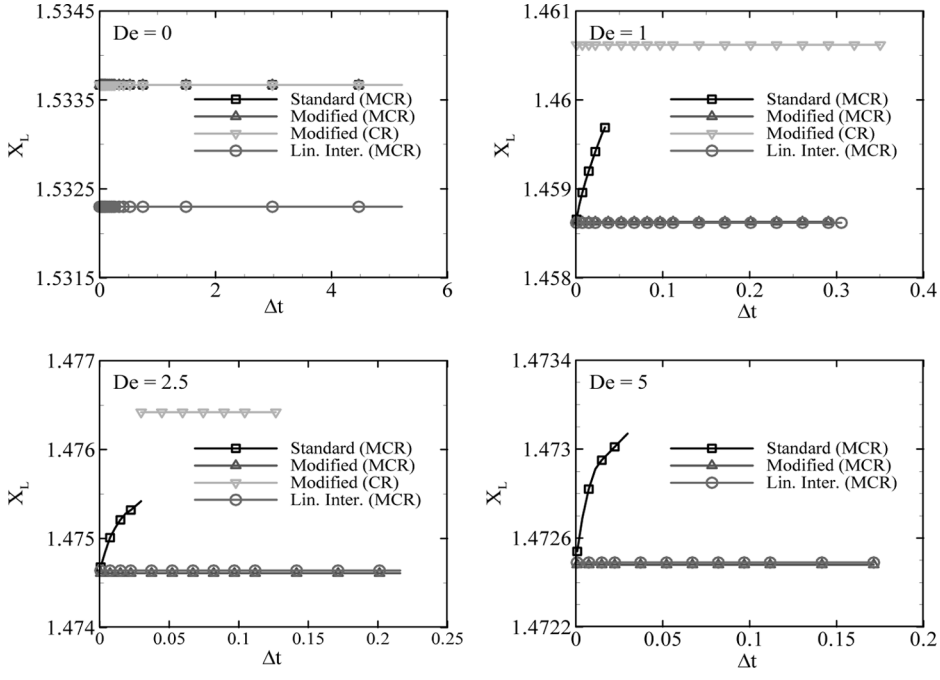

Figure 3. Variation of the horizontal recirculation length with time-step size for the formulations tested.

Downloaded By: [B-on Consortium - 2007] At: 18:42 11 January 2010

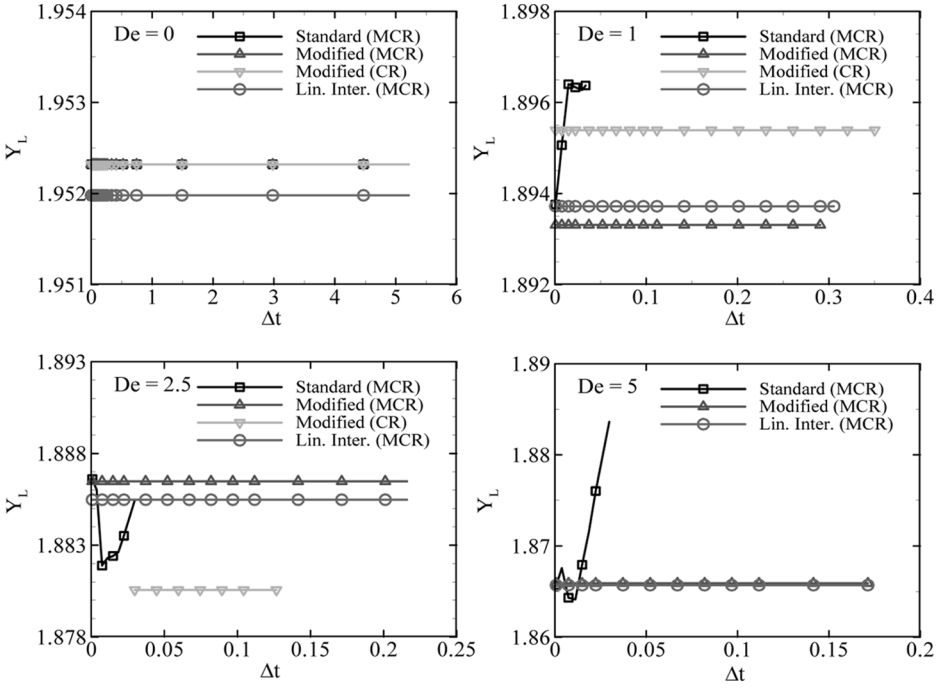

Figure 4. Variation of the vertical recirculation length with time-step size for the formulations tested.

For the Newtonian case (De = 0), Figures 3 and 4 demonstrate that both the horizontal (X_L) and vertical (Y_L) recirculation lengths are independent of the Δt employed, an expected outcome since the flux formulation *F2* [Eq. (12)] is, theoretically, invariant with respect to Δt. No formulation reveals any limitation in terms of Δt, a sign of robustness of the algorithm implementation, and simulations at higher Δt are not shown due to the considerable CPU times involved. Formulations Standard and Modified (with either the CR or MCR rheological models) yield identical results, as expected since the Modified formulation for the Newtonian case ($\lambda = 0$) simplifies, giving an equation identical to that for the Standard formulation under the same conditions: Contrast Eqs. (16) and (17) with Eq. (18), after setting $\lambda = 0$ and using the definition of a_P^{τ} from Eq. (15). We note that the Newtonian conditions are simulated by setting $\eta_s = 0$, $\eta_p = \eta_0$, and $\lambda = 0$.

For the viscoelastic cases, Figures 3 and 4 show recirculation lengths versus Δt for three Deborah numbers, and it is possible to observe some Δt dependence of the results with the Standard formulation; only for Δt tending to zero do the X_L and Y_L values tend to those predicted by the other formulations. Although the differences between the extreme values predicted by the Standard formulation for the various Δt are not that significant, being around 0.07% for X_L and 0.2% for Y_L, it is still a nuisance that is circumvented by the improved new formulation of Eq. (18). An additional problem with the Standard formulation illustrated in these plots is that convergence is only guaranteed for a small range of Δt: $0 < \Delta t < 0.023$. Both the Modified and the Linear Interpolation formulations provide results independent

Downloaded By: [B-on Consortium - 2007] At: 18:42 11 January 2010

of Δt, as expected theoretically, and are able to provide results (that is, to achieve iterative convergence) for a much wider range of time-step sizes: $0 < \Delta t < \Delta t_{\max}$; the maximum allowable time step ($\Delta t_{\max}$) diminishes with Deborah number. This is not unexpected, since viscoelastic flows are notoriously difficult to simulate successfully (e.g., [24]), especially when singular points are present within the flow domain (as the two corners at the entrance to the side branch in the T-junction geometry) and the elasticity level, measured by De, is enhanced. For the highest-elasticity case shown, $\mathrm{De} = 5$, the Modified and Linear Interpolation formulations converge up to identical time-step values, $\Delta t_{\max} = 0.17$, and the maximum variation between the vortex lengths predicted by those formulations is just 0.022% at $\mathrm{De} = 1$ and 0.011% at $\mathrm{De} = 2.5$.

Differences between the X_L and Y_L values predicted by the two constitutive models are slightly larger, as observed from Figures 3 and 4 for the MCR and CR models (both cases with the Modified formulation), but are still small on account of the similitude between those models: 0.14% in X_L and 0.11% in Y_L at $\mathrm{De} = 1$; these rise to 0.12% in X_L and 0.31% in Y_L at $\mathrm{De} = 5$. A distinguishing feature between the constitutive models is that the convergence range, in terms of Δt values for which iterative converged solutions can be achieved, is smaller for the CR and tends to become narrower as De is increased: at $\mathrm{De} = 2.5$, convergence is possible in the range $0.03 \leq \Delta t \leq 0.13$; at $\mathrm{De} = 3.8$, convergence was possible only for $\Delta t \approx 0.08$; and at larger De, numerical solutions for the CR model can no longer be achieved. Such deterioration of robustness with the CR model and the increased inability to obtain converged numerical results deserves further investigation in future studies.

A measure of robustness is provided by analyzing the number of iterations for convergence, which is roughly proportional to the computer times, as a function of the time-step size employed in the respective computations. These plots are shown in Figure 5 for the Newtonian case ($\mathrm{De} = 0$) and one viscoelastic case ($\mathrm{De} = 1$). The left-side plot, for the Newtonian flow, reveals the great difficulty of the Linear Interpolation formulation to obtain a "converged" numerical solution: The number of iterations required is much greater than for the other formulations, especially when the latter work close to the optimum time-step point corresponding to a minimum of iterations: $\Delta t_{\mathrm{opt}} \approx 0.15$.

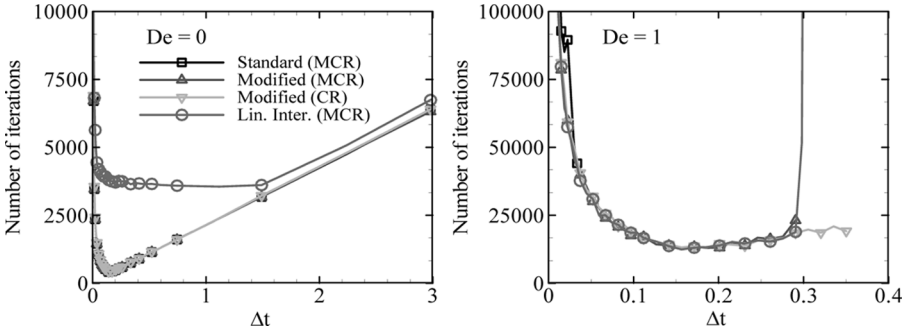

Figure 5. Variation of the number of iterations with time-step size for all formulations tested ($\mathrm{De} = 0$ and $\mathrm{De} = 1$).

Downloaded By: [B-on Consortium - 2007] At: 18:42 11 January 2010

For the viscoelastic flow case, Figure 5 shows that the total number of iterations necessary to obtain a numerical solution with the various formulations is similar, for all tested values of Δt, except the Standard formulation, which diverges at rather small Δt. We have observed similar behavior for other cases with differing values of Deborah number. Minimum values of the number of iterations occur at approximately $\Delta t \approx 0.15$, for all Deborah numbers studied, including the Newtonian case mentioned above. This value of Δt corresponds to a local Courant number ($c = u_1 \Delta t / \Delta x_{\min}$) of about $c \approx 6$, once again reflecting the benefits of the implicit algorithm, allowing Courant numbers greater than unity and hence faster convergence to steady state.

Figure 5 also shows that, contrary to the Newtonian case, the Linear Interpolation formulation does not seem to degrade the convergence rates. However, its use can be problematic because it may produce physically unrealistic solutions (with zigzag variation profiles) as reported in [1], and it is therefore not recommended in spite of its simplicity.

Downloaded By: [B-on Consortium - 2007] At: 18:42 11 January 2010

5.2. Influence of Elasticity on the Bifurcation Flow

Figure 6 depicts the evolution of the size of the horizontal and vertical recirculation eddies as a function of the Deborah number, for the formulations that are independent of the time-step value (Δt). Those eddies are illustrated in the inset of Figure 2, which shows the flow streamlines predicted with the Modified formulation for the Newtonian case ($De = 0$). The two recirculation zones formed in the main and secondary channels are reduced by about 5–6% (c.f. Figure 6) when the fluid is endowed with viscoelastic properties, at identical values of Reynolds number ($Re = 102$) and extraction ratio ($\beta = 0.7$).

From streamline plots for increasing De, not shown here for conciseness, we can determine the minimum and maximum values of the stream function ψ ($u = \partial\psi/\partial y$, $v = -\partial\psi/\partial x$), which occur at the central points of the two recirculation zones. Those values are related to the proportion of flow rate that recirculates inside each recirculation bubble, and the variation of these recirculation intensities with the Deborah number is shown in Figure 7, for the several formulations.

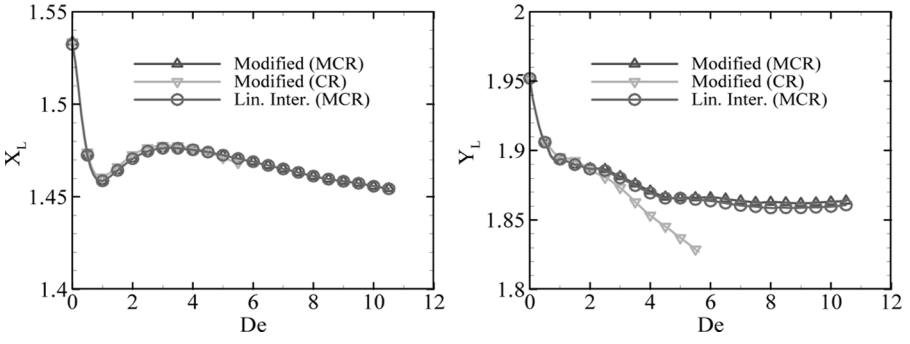

Figure 6. Variation of the horizontal (*left*) and vertical (*right*) recirculation lengths with Deborah number.

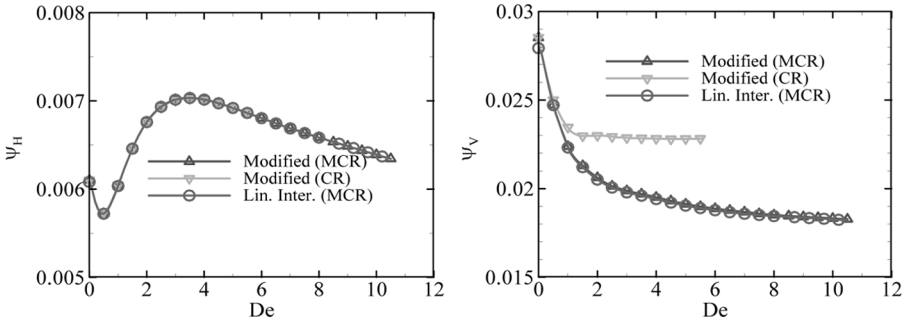

Figure 7. Variation of vortex intensity in the horizontal and vertical recirculation bubbles.

Downloaded By: [B-on Consortium - 2007] At: 18:42 11 January 2010

Figures 6 and 7 provide the main quantitative data obtained from the simulations, and from their analysis it is verified that both the length (Y_L) and the flow rate inside the vertical recirculation ($\psi_V = \psi_{\max} - 1$) tend to decrease with an increase of Deborah number. Hence, the eddy in the side branch exhibits the usual suppression of vortex activity brought about by elasticity in expansion flows [31]. On the other hand, the horizontal recirculation presents a different and more complex behavior: The length of the recirculation (X_L) initially decreases quickly with an increase of Deborah number, but then, after attaining a certain minimum size at $\mathrm{De} \approx 1$, there is an upturn and the vortex starts increasing with De, before decreasing again later, for $\mathrm{De} \gtrsim 3$, at a slower rate. The variation of the flow inside this recirculation presents nonmonotonic behavior too, akin to the X_L-versus-De variation, presenting an initial abrupt decrease with Deborah number, followed by a gradual increase up to $\mathrm{De} \approx 3.5$ and a slow decrease later. Such difference between the influence of elasticity on the horizontal and vertical bubbles, in terms of both their size and strength, are related to the extra degree of freedom introduced by the movable separation point of the horizontal recirculation. At a middle range of Deborah numbers ($\mathrm{De} \approx 1 - 3$), the point of flow separation slides upstream, allowing the recirculation in the main channel to increase in both size and intensity.

Figure 8 shows contour plots of the shear stress field in the bifurcation zone. This figure is for predictions corresponding to $\mathrm{De} = 1$ obtained with the Modified

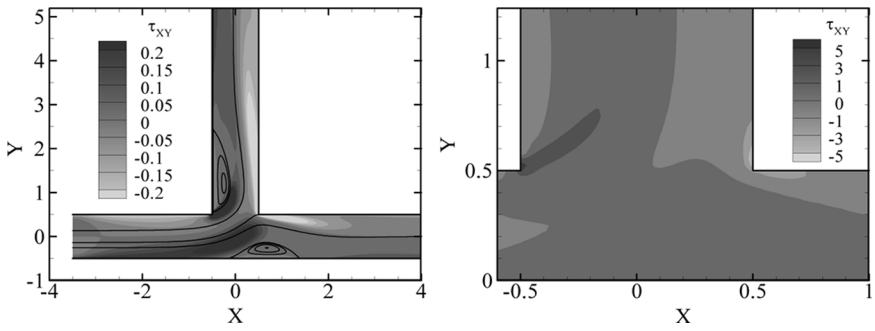

Figure 8. Contours of the shear stress component in the bifurcation zone for $\mathrm{De} = 1$.

formulation and the MCR constitutive model. It may be observed from Figure 8 that the shear stresses inside the recirculation zones are generally very low, thus inducing the possibility in corresponding blood flow of wall adhesion of platelets, red cells, and lipoids, which in turn may result in the formation of atherosclerotic plaques and thrombi. On the other hand, the zoomed detail in the right plot of Figure 8 shows the existence of very high (in modulus) shear stresses in localized regions close to the reentrant corner ($X = Y = +0.5$) and also at the wall in front of the vertical recirculation eddy and before the horizontal recirculation eddy (Figure 8, left), where the endothelium of the arteries may be damaged, thus eventually triggering vascular disease (mechanism discussed by, e.g., [22]).

6. CONCLUSIONS

Numerical simulations were conducted for flow in a two-dimensional bifurcation with Newtonian and non-Newtonian fluids in order to test several existing and a newly developed formulation for the stress calculation at control volume faces. These cell-face stresses are important to evaluate the forces acting on each control volume, as a consequence of the stress-divergence term in the momentum equations, and the new formulation produces results that are independent of the time-step value used.

The results obtained in this study show that the proposed Modified formulation, using the FENE-MCR constitutive equation, is the most versatile formulation, for both Newtonian and non-Newtonian viscoelastic flows. For all, except the Standard formulation, it was possible to obtain steady solutions independent of the time step used, in agreement with theoretical analysis. In the case of the viscoelastic flows, the formulation with Linear stress interpolation presented good results but, for the Newtonian flow case, it exhibits non-negligible convergence difficulties.

The existence of high shear stresses was confirmed in the reentrant corners of the bifurcation, as well as the existence of low shear stresses in the recirculation zones.

The new formulation proposed here for viscoelastic flows turned out to be less versatile when applied in conjunction with the FENE-CR constitutive model than with the MCR model; however, we think that the problems observed at high De are most probably due to the onset of an elastic instability, typical of high-De flows. Discrimination between rheological models was not the main objective of the present study, and therefore that issue will be further investigated in the future. Nevertheless, the Modified formulation proposed here is clearly more robust than the previous Standard formulation and provides Δt-independent numerical solutions, thus representing an important improvement in viscoelastic flow computations.

REFERENCES

1. P. J. Oliveira, F. T. Pinho, and G. A. Pinto, Numerical Simulation of Non-linear Flows with a General Collocated Finite-Volume Method, *J. Non-Newtonian Fluid Mech.*, vol. 79, pp. 1–43, 1998.
2. P. J. Oliveira and F. T. Pinho, Numerical Procedure for the Computation of Fluid Flow with Arbitrary Stress-Strain Relationships, *Numer. Heat Transfer B*, vol. 35, pp. 295–315, 1999.

Downloaded By: [B-on Consortium - 2007] At: 18:42 11 January 2010

3. C. M. Rhie and W. L. Chow, Numerical Study of the Turbulent Flow Past an Airfoil with Trailing Edge Separation, *AIAA J.*, vol. 21, pp. 1525–1532, 1983.
4. M. A. Alves, P. J. Oliveira, and F. T. Pinho, Benchmark Solutions for the Flow of Oldroyd-B and PTT Fluids in Planar Contractions, *J. Non-Newtonian. Fluid Mech.*, vol. 110, pp. 45–75, 2003.
5. S. Majumdar, Role of Underrelaxation in Momentum Interpolation for Calculation of Flow with Nonstaggered Grids, *Numer. Heat Transfer*, vol. 13, pp. 125–132, 1988.
6. T. F. Miller and F. W. Schmidt, Use of a Pressure-Weighted Interpolation Method for the Solution of the Incompressible Navier-Stokes Equations on a Nonstaggered Grid System, *Numer. Heat Transfer*, vol. 14, pp. 213–233, 1988.
7. P. J. Oliveira, Computer Modelling of Multidimensional Multiphase Flow and Application to T-junctions, Ph.D. thesis, Imperial Collage, University of London, 1992.
8. R. I. Issa and P. J. Oliveira, Numerical Prediction of Phase-Separation in Two-Phase Flow Through T-Junctions, *Comput. Fluids*, vol. 23, pp. 347–372, 1994.
9. S. K. Choi, Note on the Use of Momentum Interpolation Method for Unsteady Flows, *Numer. Heat Transfer A*, vol. 36, pp. 545–550, 1999.
10. W. Z. Shen, J. Michelsen, and J. N. Sorensen, Improved Rhie-Chow Interpolation for Unsteady Flow Computations, *AIAA J.*, vol. 39, pp. 2406–2409, 2001.
11. B. Yu, Y. Kawaguchi, W.-Q. Tao, and H. Ozoe, Checkerboard Pressure Predictions due to the Underrelaxation Factor and Time Step Size for a Nonstaggered Grid with Momentum Interpolation Method, *Numer. Heat Transfer B*, vol. 41, pp. 85–94, 2002.
12. C. Y. Gu, Computation of Flows with Large Body Forces, Proc. Numerical Methods in Laminar and Turbulent Flow, Pineridge Press, Swansea, UK, 1991.
13. J. Mencinger and I. Zun, On the Finite Volume Discretization of Discontinuous Body Force Field on Collocated Grid: Application to VOF Method, *J. Comput. Phys.*, vol. 221, pp. 524–538, 2007.
14. R. F. Kunz, B. W. Siebert, W. K. Cope, N. F. Foster, S. P. Antal, and S. M. Ettorre, A Coupled Phasic Exchange Algorithm for Three-Dimensional Multi-field Analysis of Heated Flows with Mass Transfer, *Comput. Fluids*, vol. 27, pp. 741–768, 1998.
15. P. J. Oliveira and R. I. Issa, Numerical Aspects of an Algorithm for the Eulerian Simulation of Two-Phase Flows, *Int. J. Numer. Meth. Fluids*, vol. 43, pp. 1177–1198, 2003.
16. D. Liepsch, S. Moravec, A. K. Rastogi, and N. S. Vlachos, Measurement and Calculations of Laminar Flow in a Ninety Degree Bifurcation, *J. Biomech.*, vol. 15, pp. 473–485, 1982.
17. J. M. Khodadadi, N. S. Vlachos, D. Liepsch, and S. Moravec, LDA Measurements and Numerical Prediction of Pulsatile Laminar Flow in a 90-Degree Bifurcation, *J. Biomech. Eng.*, vol. 110, pp. 129–136, 1988.
18. J. M. Khodadadi, Wall Pressure and Shear Stress Variations in a 90-Deg Bifurcation during Pulsatile Laminar Flow, *J. Fluids Eng.*, vol. 113, pp. 111–115, 1991.
19. A. I. P. Miranda, P. J. Oliveira, and F. T. Pinho, Steady and Unsteady Laminar Flows of Newtonian and Generalized Newtonian Fluids in a Planar T-junction, *Int. J. Numer. Meth, Fluids*, vol. 57, pp. 295–328, 2007.
20. R. G. Owens, A New Microstructure-Based Constitutive Model for Human Blood, *J. Non-Newtonian Fluid Mech.*, vol. 140, pp. 57–70, 2006.
21. R. B. Bird, O. Hassager, R. C. Armstrong, and C. F. Curtiss, *Dynamics of Polymeric Liquids: Kinetic Theory*, vol. II, Wiley, New York, 1987.
22. R. S. Salzar, M. J. Thubrikar, and R. T. Eppink, Pressure-Induced Mechanical Stress in the Carotid Artery Bifurcation: A Possible Correlation to Atherosclerosis, *J. Biomech.*, vol. 28, pp. 1333–1340, 1995.
23. M. D. Chilcot and J. M. Rallison, Creeping Flow of Dilute Polymer Solutions Past Cylinders and Spheres, *J. Non-Newtonian. Fluid Mech.*, vol. 29, pp. 381–432, 1988.

Downloaded By: [B-on Consortium - 2007] At: 18:42 11 January 2010

24. P. J. Coates, R. C. Armstrong, and R. A. Brown, Calculation of Steady State Viscoelastic Flow through Axisymmetric Contractions with the EEME Formulation, *J. Non-Newtonian. Fluid Mech.*, vol. 42, pp. 141–188, 1992.
25. S. V. Patankar, *Numerical Heat Transfer and Fluid Flow*, Hemisphere, New York, 1980.
26. J. H. Ferziger and M. Peric, *Computational Methods for Fluid Dynamics*, 3rd ed., Springer-Verlag, Berlin, 2002.
27. M. A. Alves, P. J. Oliveira, and F. T. Pinho, A Convergent and Universally Bounded Interpolation Scheme for the Treatment of Advection, *Int. J. Numer. Meth. Fluids*, vol. 41, pp. 47–75, 2003.
28. J. P. Van Doormaal and G. D. Raithby, Enhancements of the SIMPLE Method for Predicting Incompressible Fluid Flows, *Numer. Heat Transfer*, vol. 7, pp. 147–163, 1984.
29. B. Yu, W.-Q. Tao, J.-J. Wei, Y. Kawaguchi, T. Tagawa, and H. Ozoe, Discussion on Momentum Interpolation Method for Collocated Grids of Incompressible Flow, *Numer. Heat Transfer B*, vol. 42, pp. 141–166, 2002.
30. W. Z. Shen, J. A. Michelsen, N. N. Sørensen, and J. Nørkær Sørensen, An Improved Simplec Method on Collocated Grids for Steady and Unsteady Flow Computations, *Numer. Heat Transfer B*, vol. 43, pp. 221–239, 2003.
31. P. Townsend and K. Walters, Expansion Flows of Non-Newtonian Liquids, *Chem. Eng. Sci.*, vol. 49, pp. 749–763, 1994.

Downloaded By: [B-on Consortium - 2007] At: 18:42 11 January 2010